https://doi.org/10.53656/nat2023-1.02

Experiments

EVALUATION OF QUANTITATIVE CRITERIA FOR TRIASSIC RESERVOIRS IN THE SOUTH MANGYSHLAK BASIN

Hofmann, M.[1)], AL-Obaidi, S. H.[2)], Chang W. J.[3)]
[1)]Mining University – Saint Petersburg (Russia)
[2)]Department of Petroleum Engineering, University of Xidian (China)

Abstract. Carbonate rocks of the Triassic deposits of the South Mangyshlak basin are investigated in this paper for their boundary values, which are important for interpretation of field geophysical data as well as perforation and blasting.

Based on their lithological composition, Triassic deposits are classified as either terrigenous or carbonate reservoirs. Carbonate reservoirs are found in the Middle Triassic strata containing volcanogenic dolomite and volcanogenic limestone rocks. A complex type of reservoir characterizes these rocks: porous-fractured, porous-cavernous, and fractured. Upper Triassic sediments are formed by the intercalation of tuffaceous, siltstone-sandy, and mudstone rocks overlying Middle Triassic sedimentary rocks. Oil deposits are confined to polymictic sandstones, which are oil-saturated to varying degrees.

In order to substantiate the quantitative criteria of the reservoir, experimental studies of the core samples were carried out in the laboratory. Fluid flow studies were performed where physical and hydrodynamic characteristics were determined when oil was displaced by displacing reagents. On the basis of the parameters obtained, correlations between reservoirs and non-reservoirs were constructed. Based on relationships between reservoir properties such as porosity and permeability versus residual water content, as well as effective porosity and permeability versus dynamic porosity, the boundary values were determined. Using these results, the porosity limit for the Middle and Upper Triassic strata has been determined to be 7%, the permeability limit for the Middle Triassic has been determined to be 0.02 X 10^{-3} μm^2, and the permeability limit for the Upper Triassic has been determined to be 0.3 X 10^{-3} μm^2.

Keywords: Quantitative Criteria; Carbonate rocks; boundary values; Triassic deposits; Carbonate Rocks Reservoirs

1. Introduction

As a result of geological exploration at Mangyshlak basin during the 70s – 90s of the last century, numerous oil and gas fields were discovered with proven productivity (Li et al. 2020; Murzagaliev 1996; Kamensky, Al-Obaidi

& Khalaf 2020; Sobornov 1995).Triassic carbonate reservoirs in the basin exhibit a number of characteristics, including complex pore structures, high heterogeneity in flow and reservoir properties, variety of rock compositions, and many others (Timurziev 1984; Al-Obaidi & Khalaf 2017; Feyzullayev, Kadirov & Kadyrov 2016; Al-Obaidi, Kamensky & Hofmann 2010). These characteristics complicate the interpretation of field geophysical data, the selection of reservoirs, and the design of development models.

To identify carbonate reservoirs of Triassic deposits using well logging methods, it is difficult to identify the boundaries of the reservoirs using qualitative features due to the complex structure of the deposits and a number of factors that negatively affect the curves. Therefore, the technology of identifying reservoirs according to quantitative criteria that determine the "reservoir-non-reservoir" boundary at the static level is necessary to clarify the interpretation (Huang et al. 2022; Ulmishek 2001; Al-Obaidi 2022; Soroush et al. 2021). In order to determine the boundary values, correlation dependencies were constructed based on the parameters obtained from special laboratory core tests.

2. Lithological and petrographic characteristics of Triassic carbonate reservoirs

2. 1 Lower Triassic deposits (T1)

The carbonate-terrigenous sequence of the Lower Triassic (T1), which lies at the base of the oil and gas complex, is composed of rhythmically interbedded siltstones, sandstones, mudstones, and limestones. Due to numerous ammonite finds in the carbonate-terrigenous sequence, the age of the carbonate-terrigenous sequence has been determined to be late Olenekian (Rabinovich, Palamar & Popkov 1983; Al-Obaidi, Hofmann & Kamensky 2010; Gurbanov 2004). The reservoirs (porous-fractured) are composed of arkosic sandstones with effective porosity from 8 to 18%, fracture permeability up to 6.5×10^{-3} μm^2, and porous permeability from 0.1 to 141×10^{-3} μm^2 (Kettanah 2003; Al-Obaidi, Patkin & Guliaeva 2003). The productivity of the stratum has been established at the Tasbulat and South Zhetybai fields and weak oil inflows have been obtained at the Uzen, West Tasbulat, and West Tenge fields. The sequence is absent within the Beke-Bashkuduk swell (the western part, in the areas of Saura and Segenda, and the eastern part of Sokko, Shalabai and Senek), the northern part of the Uzen uplift, in the southwest of the Zhetybay-Uzen step (northwestern Zhetybay, Pridorozhnaya), and in the North Karagiinskaya area (Fig. 1).

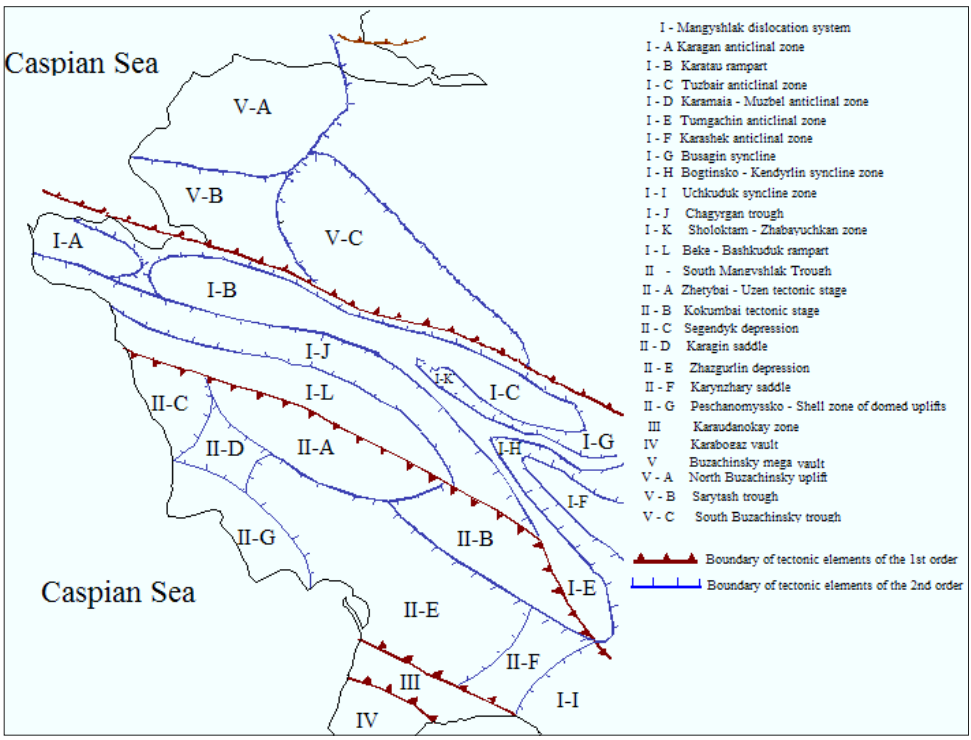

Figure 1. Mangyshlak Tectonic Scheme

2. 2. Middle Triassic deposits (T2)

The Middle Triassic deposits (T2) consist of a volcanic-carbonate grey-colored formation, which accumulated under the conditions of a marine brackish-water basin and humid conditions. The formation consists of three lithological layers (from bottom to top):

– volcanogenic-dolomitic;
– volcanogenic-limestone;
– volcanic-argillic.

A volcanic-dolomite layer lies on the underlying Lower Triassic. The composition of this rock is characterized by the wide development of oolitic-cloddy tuffs, tuffites, tuff mudstones, and clastic polydetrital limestones. Due to the development of carbonate rocks, which can be easily leached, reservoir properties such as effective porosity and permeability are high. It has a porosity of up to 28% and a permeability of $115x10^{-3}$ μm^2 (Kulumbetova, Nursultanova & Mailybayev 2019; Zholtayev & Kuandykov 1999; Kamensky & Al-Obaidi 2022).

The void space is represented by intra-form isolated pores formed as a result of calcite leaching. The inter-formal space is filled with clear-crystalline calcite.

Immediately above the section is a volcanogenic limestone sequence, consisting of limestones with rare interlayers of dolomites, tuffites, tuff sandstones, mudstones and siltstones. The limestones are highly bituminized, which causes the black color of the rocks. There is a significant reduction in reservoir properties due to the widespread development of tuffaceous rocks.

The upper part of the Middle Triassic section - volcanogenic-argillite sequence is composed mainly of mudstones with an admixture of tuffaceous material and thin interlayers of carbonate rocks (lower part) and siltstones (upper part). The rocks are characterized by low reservoir properties and are often taken as a seal for hydrocarbon deposits confined to the carbonate layer (Galkin et al. 2005; Kurmanov 1999).

Upper Triassic deposits (T3)

There is a coarse-grained unit at the base of the stratum with a thickness of 40 to 70 m with the following reservoir properties; effective porosity up to 20%, permeability of 10×10^{-3} μm^2 (Windley et al. 2007; Al-Obaidi 2016). The overlying part of the section is composed of inequigranular tuff sandstones, tuff siltstones, and tuff mudstones (Kiritchkova & Nosova 2014).

The total thickness of the Middle Triassic deposits within the South Mangyshlak reaches 600-650 m (Qin et al. 2015; Smirnov & Al-Obaidi 2008).

3. Methodology and materials

To assess the boundary values, studies were carried out on the selected core in the period 2010-2019 (Shilanov 2018; Gaafar, Tewari & Zain 2015; Hofmann, Al-Obaidi & Kamensky 2021). General information on sampling for the core studies is presented in Table 1.

To assess the boundary values of porosity and permeability properties, a 2-phase flow unit was used, the main elements of which are:

1. Vertically positioned core holder designed for core samples with a diameter of 1½ inches and a length of 12 inches.
2. Vertically positioned X-ray system for continuous core scanning and real-time determination of water-oil saturation.
3. A set of precision pumps and temperature sensors for fluid flow under thermobaric conditions.
4. Transducer module for differential pressure detection.

Table 1. Detailed information on selected samples

Field/Well	Horizon	Lithology	Number of experiments
X-10	T3, Basal	Fine-grained sandstone	2
X-3	T3, Basal	Fine-grained sandstone	2
Y-9	T3, Basal	Tuff sandstone	2
Y-40	T3, Basal	Tuff sandstone	2
X-15	T2, volcanic-dolomitic	Calcareous dolomite	1
X-27	T2, volcanic-dolomitic	Clastic dolomite, cavernous	1
Y-40	T2	Tuff siltstone	1

3. 1. Preparation of core samples

The preparation of core samples for experimental studies included several stages.

Stage 1: Drilling samples with a diameter of 1½ inches were collected from the working part of the sawn core.

Samples were extracted in Soxhlet reflux devices (Kløv et al. 2003; Al-Obaidi 2020), using toluene as a solvent, then a mixture of chloroform and methanol in a ratio of 9:1, respectively. For standard and special core studies, samples were dried and placed in a desiccator with silica gel to prevent moisture from adsorbing from the air.

Stage 2: Matrix density, porosity, and absolute permeability were determined by standard core testing. To measure the matrix density of grains, coefficients of effective porosity, and absolute permeability of rocks, an UltraPoroPerm-500 device from Core Laboratories Instruments (CLI) was used (Alcaíno-Olivares et al. 2022; Joseph, Gunda & Mitra 2013; Al-Obaidi & Guliaeva 2002). The operating principle of the porosimeter is based on the use of the Boyle-Mariotte law. Absolute gas permeability was measured during steady-state flow using a standard Hassler core holder by injection of nitrogen gas. The operating principle of the permeameter is based on the use of Darcy's law (Nijp et al. 2017; Chang, Al-Obaidi & Khalaf 2021).

A hydrostatic pressure of 400 psi was applied to the side surface of the sample. The absolute permeability of the rock was automatically calculated when the airflow followed the Darcy law.

Stage 3: In addition to the saturation of core samples using an auto-saturator with a reservoir water model, measurements were made of partial and residual water saturation coefficients, relative phase permeability of oil and water, and residual oil saturation. Before the start of the experiments, the selected sam-

ples were saturated in a vacuum saturator with a reservoir water model (RWM) using a prepared synthetic solution of the NaCl type with a mineralization of 20 – 40 g/l.

The core samples, pre-saturated with RWM, were placed in a specially designed gamma-ray-transmitting core holder, where reservoir pressure was created. First, the water phase permeability of the rock was determined at 100% RWM saturation. Then, without removing the sample from the core holder, water was displaced under reservoir conditions using crude oil, and the coefficients of residual water saturation and oil phase permeability were determined. The coefficient of residual water saturation of core samples was determined from the results of X-ray scanning (Withjack, Devier & Michael 2003).

Steady-state studies

As soon as the core samples had been prepared, oil and water were injected simultaneously in different proportions: 75/1, 25/1, 5/1, 1/1, and 1/10. Each subsequent batch injection was performed after the stabilization of the differential pressure.

With the aid of an X-ray scanner, the effective permeability of each phase and water saturation of the samples were measured at each stage of the experiment.

After batch injection of two phases, water injection equal to 25 times the pore volume was performed until residual oil saturation was achieved, and oil phase permeability was determined.

The water saturation of the sample extracted from the core holder was also determined by the extraction method in the Dean-Stark apparatus (Handwerger et al. 2012; Liu et al. 2022).

To determine the oil phase permeability, the samples were additionally cleaned, dried, and saturated with crude oil. Then, the samples were placed in a core holder, after which crude oil was injected and the oil permeability coefficient was determined at 100% oil saturation.

The results of the experiments performed are presented in Table. 2.

Table 2. Results of special core studies

Indicators	**Unit of meas.**	**Experiment**							
		№ 1	**№ 2**	**№ 3**	**№ 4**	**№ 5**	**№ 6**	**№ 7**	**№ 8**
Field / well		X-10		X-3		Y-9		Y-40	
Laboratory № of the sample		26	22	5	7	225	242	219	220
Lithology		Sand-stone	Sand-stone	Sand-stone	Sand-stone	Tuff sandstone	Tuff sandstone	Tuff sandstone	Tuff sandstone

Depth	m	3256,2	3262,12	3699,54	3698,87	2962,03	3037,31	3703,05	3703,23
Effective porosity	Fraction	0,155	0,175	0,143	0,140	0,246	0,138	0,180	0,182
Absolute Permeability	$\times 10^{-3}$ μm^2	107,9	206,9	32,0	31,6	23,1	1,4	51,1	29,1
Density of formation water	g/cm^3	1,056	1,056	1,056	1,056	1,061	1,061	1,061	1,061
Oil viscosity	mPa.s	0,560	0,560	0,560	0,560	1	1	1	1
Oil density	g/cm^3	0,758	0,758	0,758	0,758	0,798	0,798	0,798	0,798
General mineralization	g/l	28	28	28	28	21	21	21	21
Residual water saturation	Fraction	0,220	0,230	0,276	0,262	0,384	0,470	0,334	0,391
Residual oil saturation	Fraction	0,356	0,325	0,349	0,355	0,345	0,349	0,366	0,351
Water permeability at residual oil	$\times 10^{-3}$ μm^2	5,676	5,860	8,022	7,977	6,545	0,216	17,556	5,470
Oil permeability	$\times 10^{-3}$ μm^2	13,583	13,292	4,920	5,687	-	-	-	-
Oil permeability at residual water	$\times 10^{-3}$ μm^2	5,988	5,860	4,305	4,399	15,620	1,010	42,510	18,950
Oil displacement coefficient	Fraction	0,539	0,578	0,519	0,519	0,441	0,273	0,450	0,424
Experiment temperature	°C	130,6	130,6	130,6	130,6	115	115	115	115

4. Results and discussion

According to the results of the studies, Fig. 2 presents graphs of relative permeability for both water and oil. The following conclusions can be drawn from these graphs of relative permeability:

Residual oil saturation of rocks varies within 32.5 – 36.6%.

Residual water saturation within 22.0 – 47.0%.

Oil displacement ratio is 27.3 – 57.8%.

The limiting value of the relative permeability of water is 0.2 – 0.4 units, indicating that the rocks are hydrophilic.

According to the results of special studies conducted, residual water saturation and oil saturation were determined. The dynamic porosity of rocks was calculated using the following expression:

$$\varphi_D = \varphi_e * (1 - S_w - S_o) \quad (1)$$

Where φ_D – Dynamic porosity; φ_e – Effective porosity of rocks by helium; S_w – Residual water saturation; S_o – Residual oil saturation.

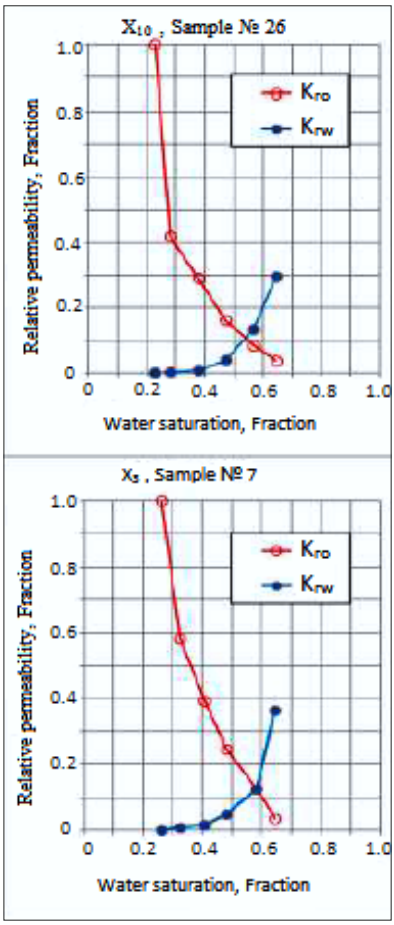
X10 , Sample № 26
Kro
Krw
Relative permeability, Fraction
Water saturation, Fraction
X3 , Sample № 7
Kro
Krw
Relative permeability, Fraction
Water saturation, Fraction

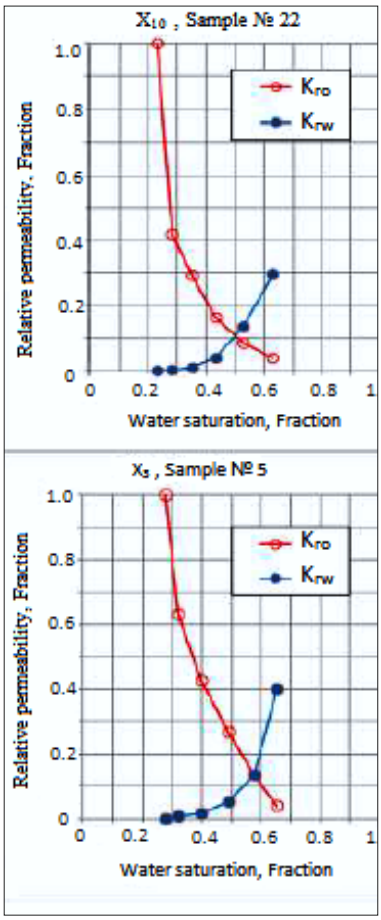
X10 , Sample № 22
Kro
Krw
Relative permeability, Fraction
Water saturation, Fraction
X3 , Sample № 5
Kro
Krw
Relative permeability, Fraction
Water saturation, Fraction

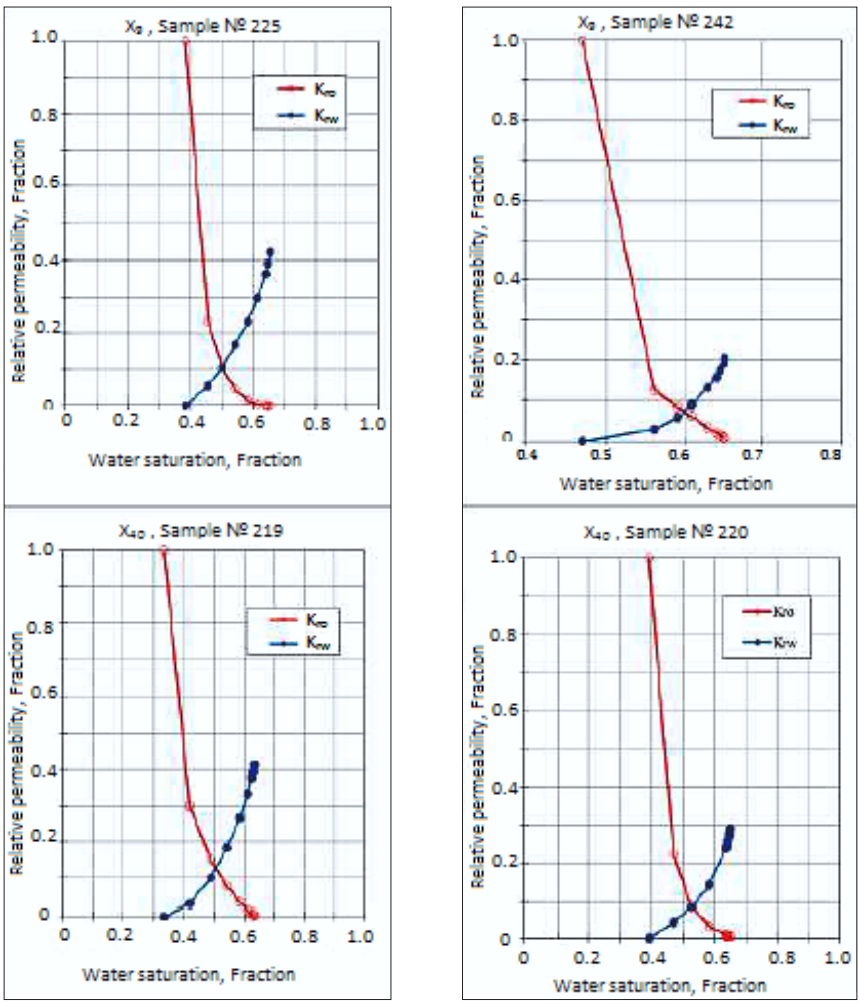

Figure 2. The relative permeability curves for oil and water

As the residual water-oil saturation is considered, the dynamic porosity characterizes the capacitive and flow properties of the formation. When the rock has a dynamic porosity of 0%, the residual water-oil saturations fill the entire pore space, making it a non-reservoir. It is possible to estimate the boundary values of Upper Triassic productive reservoirs using the constructed relationships "dynamic porosity – effective porosity" and "dynamic porosity-absolute permeability" presented in Figure 3 and Figure 4.

Thus, the limit values for Upper Triassic reservoirs are defined as:
1. The porosity boundary value is 7%.
2. The value of the boundary permeability is 0.3 x 10^{-3} μm^2.

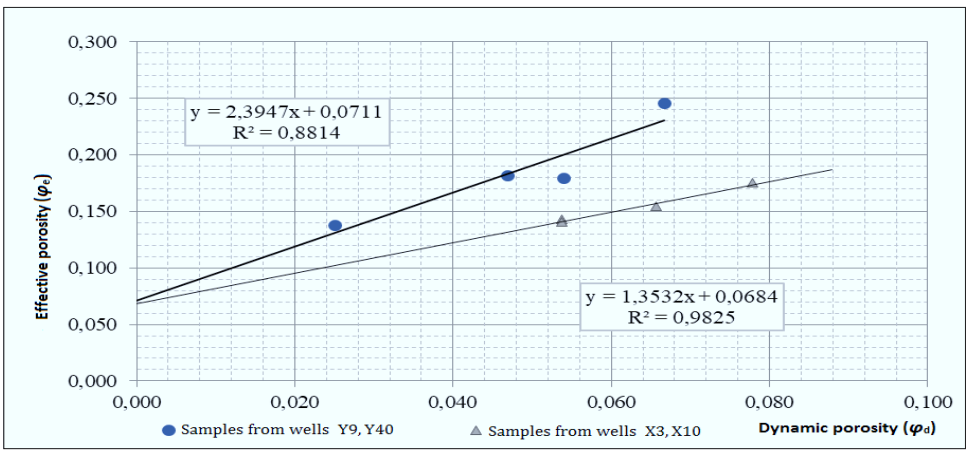

Figure 3. The relationship between dynamic porosity and effective porosity

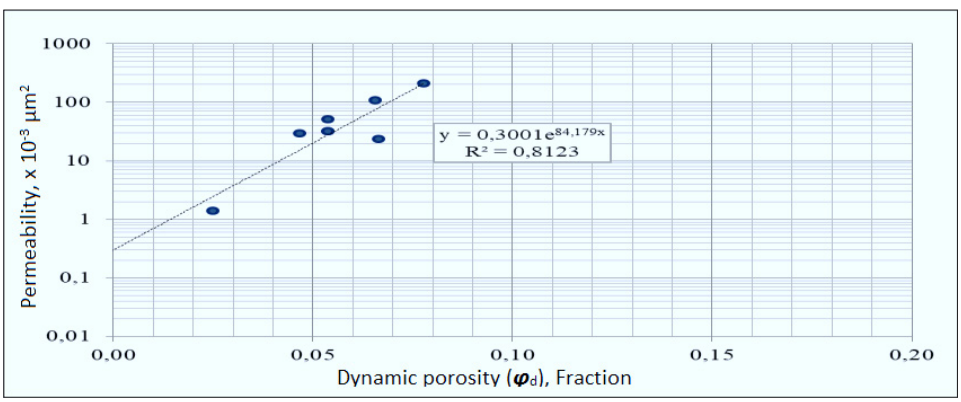

Figure 4. The relationship between dynamic porosity and absolute permeability

The Middle Triassic rocks were also studied in depth. Samples were taken from different wells and fields.

However, when performing studies for rocks from several fields, when water was injected, the differential pressure increased to 3200 psi, and the water permeability was less than 0.1 × 10^{-3} μm^2, which did not allow further studies. This factor may be related to the hydrophobicity of the rocks. A summary of the initial information and results can be found in Table 3.

Table 3. Results of special core studies

Indicators	Unit of measurement	Experiment		
		№ 5	**№ 6**	**№ 7**
Field / well		X-15	X-27	Y-40
Laboratory № of the sample		259A	161	2
Lithology		Calcareous dolomite	Dolomite	Tuff siltstone
Depth	m	2944,91	3789,55	3588,31
Effective porosity	Fraction	0,237	0,153	0,103
Absolute Permeability	$\times 10^{-3}$ μm^2	63,7	0,63	0,237
Density of formation water	g/cm^3	1,061	1,06	1,061
Oil viscosity	mPa.s	1	1	1
Oil density	g/cm^3	0,798	0,8	0,798
General mineralization	g/l	24,5	21	21
Residual water saturation	Fraction	0,27038	0,453	0,35
Residual oil saturation	Fraction	0,464	-	-
Oil permeability	$\times 10^{-3}$ μm^2	4,81	0,11	0,05
Oil permeability at residual water	$\times 10^{-3}$ μm^2	3,76	-	-
Oil displacement coefficient	Fraction	0,364	-	-
Experiment Temperature	°C	115	115	115

For a more reliable determination of the hydrophobization of rocks, the most permeable laboratory sample No. 259A (63.7×10^{-3} μm^2), represented by calcareous dolomite, was chosen. The studies were carried out in a steady-state mode. The

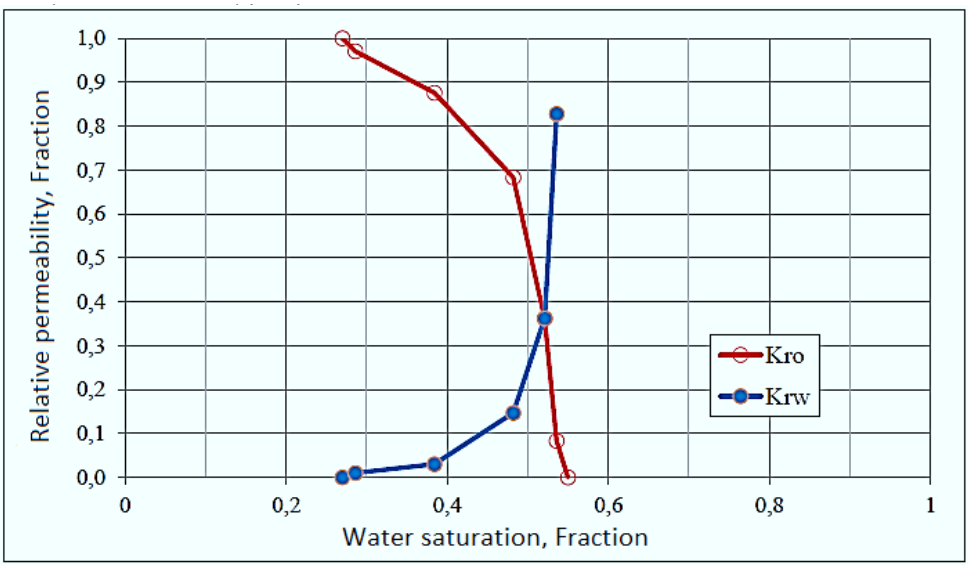

Figure 5. The relative permeability curves for oil and water

As a result of the relationship between the relative permeability of oil and water, we can conclude the following:

Residual oil saturation of rocks is high – 46.4%;

Residual water saturation – 27.0%;

Oil displacement ratio is only 36.4%;

The limiting value of the water's relative permeability is 0.83 units, which indicates the hydrophobicity of the rocks.

To determine the boundary value of the effective porosity of rocks, instead of determining the residual oil saturation and, accordingly, dynamic porosity, a mass determination of capillary pressure was performed under reservoir conditions using a high-speed centrifuge.

The studies involved 124 samples selected in 2012 – 2015 (Gurbanov & Zinalova 2018). A maximum capillary pressure of 215 psi was used to determine residual water saturation. The obtained values of residual water saturation are compared with effective porosity. The dependencies are shown in Fig. 6 and Fig. 7.

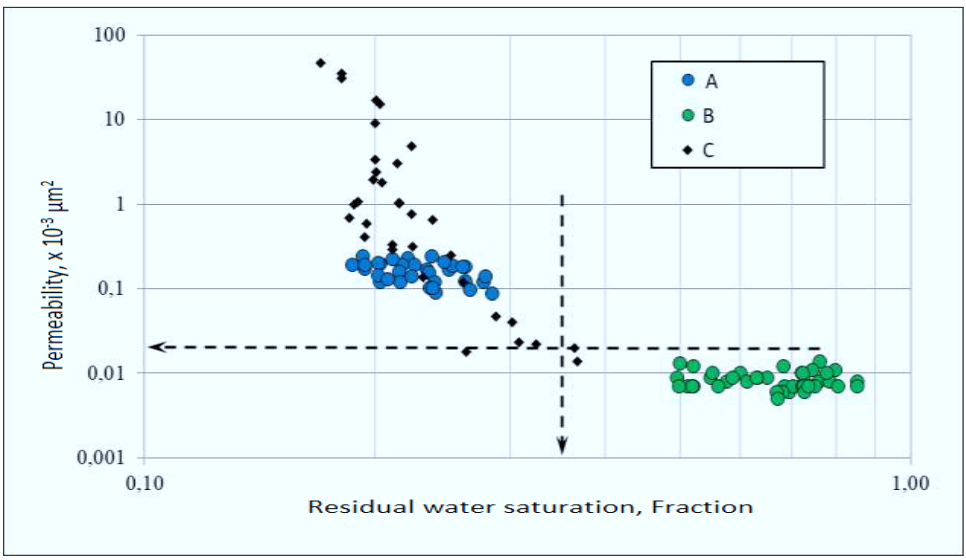

Figure 6. The relationship between the absolute permeability and residual water saturation

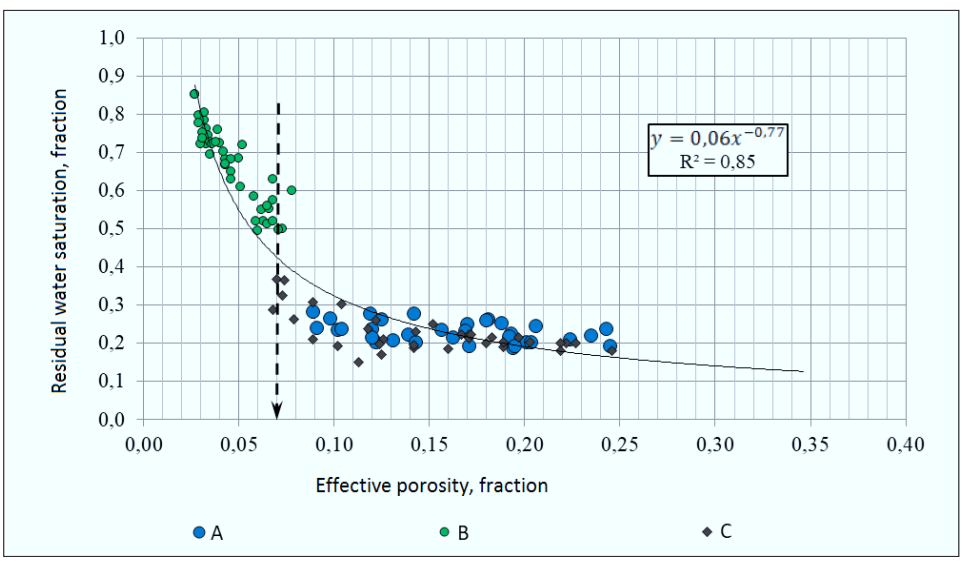

Figure 7. The relationship between the effective porosity and residual water saturation

According to the constructed dependencies, it can be seen that with a residual water saturation of more than 35%, the reservoir properties of rocks deteriorate, the fluid occupies the entire pore space, and the rock becomes a non-reservoir.

Thus, the defined limit values for volcanic-carbonate rocks of the Middle Triassic are as follows:

1. The porosity boundary value is 7%.
2. The value of the boundary permeability is 0.02 x 10^{-3} μm^2.

The reliability of reservoir properties determination in the course of well-logging data interpretation depends on the reliability of established petrophysical relationships and parameters. The quality of the core analysis carried out in the 80s does not allow today to use the results of these analyzes to build petrophysical relationships for the following reasons:

1. A low level of core recovery.
2. The lack of results from the profile studies intended to link the core to the rock section.
3. Lack of uniform sampling of cylindrical samples from all intervals, including low-permeability and non-reservoirs.
4. Insufficiency of studies - the lack of a set of studies on the same samples to establish the closeness of relationships between various parameters.

Consequently, the selection of cores and the study of reservoir properties of rocks should be continued.

5. Conclusions

Experimental analyses of the core samples were conducted in the laboratory in order to substantiate the quantitative criteria of the reservoir. By analysing the parameters, correlations were constructed between reservoirs and non-reservoirs. Boundary values were determined by analysing the relationships between reservoir properties, such as porosity and permeability, and residual water content. Based on the results of this work, the porosity limit for the Middle and Upper Triassic strata is 7%, the permeability limit for the Middle Triassic is 0.02 X 10^{-3} μm^2, and the permeability limit for the Upper Triassic is 0.3 X 10^{-3} μm^2. The use of the obtained boundary values contributes to the identification of complex carbonate reservoirs using both qualitative and quantitative features based on the difference in reservoir properties of reservoir rocks and host rocks. Since cores are being taken from new wells and various fields, the study of boundary values needs to be continued.

REFERENCES

ALCAÍNO-OLIVARES, R. et al. 2022. Rock mechanical laboratory testing of Thebes Limestone Formation (Member I), Valley of the Kings, Luxor, Egypt. *Geotechnics*. **2**(4), 825 – 854. https://doi.org/10.3390/geotechnics2040040.

AL-OBAIDI, S. H. & GULIAEVA, N., 2002. Determination of flow and volumetric properties of core samples using laboratory NMR relaxometry. *JoPET* **1**(2), 20 – 23.

AL-OBAIDI, S. H. & KAMENSKY, I. P., 2022. Express study of rheological properties and group composition of oil and condensate using nuclear magnetic resonance –relaxometry. *J Oil Gas n Coal Tech*. **4**(1):102, https://doi.org/10.36266/OJOGCT/102.

AL-OBAIDI, S. H. & KHALAF, F. H., 2017. Acoustic logging methods in fractured and porous formations. *J Geol Geophys*. **6**: 293. doi: 10.4172/2381-8719.1000293.

AL-OBAIDI, S. H. 2020. Comparison of different logging techniques for porosity determination to evaluate water saturation. *EngrXiv*. https://doi.org/10.31224/osf.io/fvj9u.

AL-OBAIDI, S. H., 2016. Improve the efficiency of the study of complex reservoirs and hydrocarbon deposits – East Baghdad field. *International journal of scientific & technology research*. **5**(8), 129 – 131.

AL-OBAIDI, S. H., 2022. Investigation of rheological properties of heavy oil deposits. *In: Advances in Geophysics, Tectonics and Petroleum Geosciences. CAJG 2019. Advances in Science, Technology & Innovation. Springer, Cham*. https://doi.org/10.1007/978-3-030-73026-0_92.

AL-OBAIDI, S. H., KAMENSKY, I. P. & HOFMANN, M., 2010. Changes in the physical properties of hydrocarbon reservoir as a result of an increase in the effective pressure during the development of the field. *EngrXiv*. February 18. doi:10.31224/osf.io/hy6pa.

AL-OBAIDI, S. H., PATKIN, A. A. & GULIAEVA, N. I., 2003. Advance use for the NMR relaxometry to investigate reservoir rocks. *JoPET*. **2**(3), 45 – 48.

CHANG, W., AL-OBAIDI, S. H & KHALAF, F., 2021. Determination of the upper limit up to which the linear flow law (Darcy's Law) can be applied. *Journal of Xidian University*. **15**(6), 277 – 286, doi: 10.37896/jxu15.6/029.

FEYZULLAYEV, A. A., KADIROV, F. A. & KADYROV, A. G., 2016. Tectono-geophysical model of the Southern Caspian in the context of the presence of oil and gas. Izv., *Phys. Solid Earth*. **52**, 912 – 922. https://doi.org/10.1134/S1069351316050049.

GAAFAR, G. R., TEWARI, R. D. & ZAIN Z. MD., 2015. Overview of advancement in core analysis and its importance in reservoir characterisation for maximising recovery. *Paper presented at the SPE Asia Pacific Enhanced Oil Recovery Conference, Kuala Lumpur, Malaysia, August*. doi: https://doi.org/10.2118/174583-MS.

GALKIN, A. et al., 2005. Dependences of reservoir oil properties on surface oil. *Jo Pet. Eng. Emerg*. (5), 74 – 7.

GURBANOV, V. S. & ZINALOVA, G. D., 2018. Reservoir properties of carbonate rocks of Triassic Deposits of Southern Mangistau. *Perm Journal of Petroleum and Mining Engineering*. **17**(1), 17 – 25. doi: 10.15593/2224-9923/2018.1.2.

GURBANOV, V. S., 2004. Lithostratigraphic characteristic and lithology of Triassic–Paleozoic rocks of Southern Mangyshlak. *Lithology and Mineral Resources*. **39**(6), 541 – 554. doi: 10.1023/B:LIMI.0000046957.60658.03.

HANDWERGER, D. A. et al., 2012. Reconciling retort versus dean stark measurements on tight shales. *Paper presented at the SPE Annual Technical Conference and Exhibition*, *San Antonio, Texas, USA, October*. doi: https://doi.org/10.2118/159976-MS.

HOFMANN, M., AL-OBAIDI, S. H. & HUSSEIN, K.F. 2022. Modeling and monitoring the development of an oil field under conditions of mass hydraulic fracturing. *Trends in Sciences*. **19**(8), 3436. https://doi.org/10.48048/tis.2022.3436.

HOFMANN, M., AL-OBAIDI, S. H. & KAMENSKY, I. P., 2021. Calculation method for determining the gas flow rate needed for liquid removal from the bottom of the wellbore. *J Geol Geophys*. **10**(5), 1 – 5.

HUANG, Y., ET AL., 2022. Assessing the geothermal resource potential of an active oil field by integrating a 3D geological model with the hydro-thermal coupled simulation. *Front. Earth Sci*. 9:787057. doi: 10.3389/feart.2021.

JOSEPH, J., GUNDA, N. S. K. & MITRA, S. K., 2013. On-chip porous media: Porosity and permeability measurements. *Chemical Engineering Science*. (99), 274 – 283. ISSN 0009-2509. https://doi.org/10.1016/j.ces.2013.05.065.

KAMENSKY, I. P., AL-OBAIDI, S. H. & KHALAF, F. H., 2020. Scale effect in laboratory determination of the properties of complex carbonate reservoirs. *International Research Journal of Modernization in Engineering Technology and Science*. **2**(11), 1 – 6.

KETTANAH, Y. A., 2003. Book Review. *Energy Sources*. 25:11, 1113 – 1117, doi: 10.1080/00908310390241091.

KIRITCHKOVA, A. I. & NOSOVA, N. V., 2014. The Lower Jurassic of the Eastern Caspian region and the Middle Caspian Basin: Lithology, facies, taphonomy. *Stratigr. Geol. Correl*. (22), 479 – 493. https://doi.org/10.1134/S0869593814050050.

KLØV, T. ET AL., 2003. Pore-to-Field Scale Modeling of WAG. *Paper presented at the SPE Annual Technical Conference and Exhibition, Denver, Colorado, October.* doi: https://doi.org/10.2118/84549-MS.

KULUMBETOVA, G. Y., NURSULTANOVA, S. G. & MAILYBAYEV, R. M., 2019. Lithological types and reservoir properties of KT-II reservoir on the Eastern edge of Pre-Caspian Basin. *International Journal of Engineering Research and Technology*. **12**(8), 1335 – 1340. ISSN 0974-3154.

KURMANOV, S., 1999. Carbonate sediments of the Pre-Caspian Basin. *Geology of Kazakhstan.* (4), 67 – 76. [In Russian]

LI, W. ET AL., 2020. Pore-throat structure characteristics and its impact on the porosity and permeability relationship of Carboniferous carbonate reservoirs in eastern edge of Pre-Caspian Basin. *Petroleum Exploration and Development*. **47**(5), 1027 – 1041, ISSN 1876-3804, https://doi.org/10.1016/S1876-3804(20)60114-8.

LIU, C. ET AL., 2022. Study and choice of water saturation test method for tight sandstone gas reservoirs. *Front. Phys*. 10:833940. doi: 10.3389/fphy.2022.833940.

MURZAGALIEV, D. M., 1996. Rifting and petroleum productivity of Mangyshlak. *Geologiya Nefti & Gaza* (5), 36 – 39. [In Russian]

NIJP, J. J., et al., 2017. A modification of the constant-head permeameter to measure saturated hydraulic conductivity of highly permeable media. *MethodsX* (4), 134 – 142. doi: 10.1016/j.mex.2017.02.002.

QIN, R. B. ET AL., 2015. Influential factors of pore structure and quantitative evaluation of reservoir parameters in carbonate reservoirs. *Earth Science Frontiers*. **22**(1): 251 – 259.

RABINOVICH, A. A, PALAMAR, V. P. & POPKOV, V. I., 1983. *Basic principles of formation of oil and gas deposits*. Nauka. Moscow (265). UDC: 553.98.061.3.

SHILANOV, N. S., 2018. Evaluation of the oil and gas potential of the Triassic-Paleozoic deposits of the South Mangyshlak on the basis of complex data of geological and geophysical studies. *Dissertation for the degree of Doctor of Philosophy in Earth Sciences, Baku*. 176 pages, p. 102.

SMIRNOV, V. & AL-OBAIDI, S., 2008. Innovative methods of enhanced oil recovery. *Oil Gas Res*. 1: e101. doi: 10.4172/2472-0518.1000e10.

SOBORNOV, K. O., 1995. Geologic framework of the petroleum productive thrust belt of eastern Caucasus, *Geologiya Nefti & Gaza* (10), 16 – 21. [In Russian]

SOROUSH, M., et al., 2021. Challenges and potentials for sand and flow control and management in the sandstone oil fields of Kazakhstan: A literature review. *SPE Drill & Compl*. **36**(01), 208 – 231. Paper Number: SPE-199247-PA. https://doi.org/10.2118/199247-PA.

TIMURZIEV, A. I., 1984. Characteristics of reservoir rocks and hydrocarbon pools in low permeable sections and improvement of methods for their prediction, *Geologiya Nefti & Gaza* (11), 49 – 54. [In Russian]

ULMISHEK, G. F., 2001. Petroleum geology and resources of the Middle Caspian Basin, former Soviet Union. *US Department of the Interior, US Geological Survey* (2201).

WINDLEY, B. F., ET AL., 2007. Tectonic models for accretion of the Central Asian Orogenic Belt. *Journal of the Geological Society*. (164), 31 – 47.

WITHJACK, E. M., DEVIER, C., & MICHAEL, G., 2003. The role of X-Ray computed tomography in core analysis. *Paper presented at the SPE Western Regional/AAPG Pacific Section Joint Meeting, Long Beach, California, May*. doi: https://doi.org/10.2118/83467-MS.

ZHOLTAYEV, G. Z. & KUANDYKOV, B. M., 1999. Geodynamic structural model of the south of Eurasia. *Oil and Gas*. (2), 62 – 74.

✉ **Prof. Dr. M. Hofmann**
ORCID iD: 0000-0001-5889-5351
Department of Petroleum Engineering
Mining University, Russia
E-mail: hof620929@gmail.com

✉ **Prof. Dr. S. H. Al-Obaidi**
ORCID iD: 0000-0003-0377-0855
Department of Petroleum Engineering
Mining University, Russia
E-mail: drsudad@gmail.com

✉ **Dr. W. Chang, Assoc. Prof.**
ORCID iD: 0000-0002-5457-2923
Department of Petroleum Engineering
University of Xidian
Xi'an, Shaanxi 710126, China
E-mail: changwj962@gmail.com